Anion Exchange in Alkyl−Zirconocene Borate Ion Pairs. Are Solvated Alkyl−Zirconocene Cations Relevant Intermediates?

Stefan Beck, Susanna Lieber, Frank Schaper, Armin Geyer, and Hans-Herbert Brintzinger*

Contribution from the Fachbereich Chemie, Universität Konstanz, D-78457 Konstanz, Germany

Received September 28, 2000. Revised Manuscript Received November 30, 2000

Abstract: Ion pairs of the type $Cp^x_2ZrMe^+\cdots A^-$ containing various *ansa*-zirconocene methyl cations in contact with Me-$B(C_6F_5)_3^-$ or $B(C_6F_5)_4^-$ anions have been studied with regard to their anion exchange kinetics by 2D-NMR methods in benzene or toluene solutions. The results—acceleration of anion exchange by added $Li^+\cdots Me-B(C_6F_5)_3^-$, substantial nonproductive exchange between added and Zr-bound Me-$B(C_6F_5)_3^-$ anions, an increase of exchange rates at increased zirconocene concentrations, and the exclusively entropic origin of this rate increase—all indicate that anion exchange occurs by way of ion quadruples or higher ionic aggregates, rather than via dissociation to solvent-separated ions. These findings imply that solvent-separated (i.e. anion-free) alkyl zirconocene cations are unlikely to be relevant intermediates in reaction systems containing $Cp^x_2ZrMe^+\cdots A^-$ ion pairs and, hence, also in zirconocene-based catalyst systems for the polymerization of α-olefins.

Introduction

Alkyl zirconocene cations $Cp^x_2ZrR^+$, where Cp^x_2Zr is a substituted and/or bridged zirconocene unit and R is a methyl or a polymeryl group, are assumed to be the active species in metallocene-catalyzed olefin polymerizations.[1] They are thought to arise by dissociation of a weakly coordinating anion A^- from an ion pair $Cp^*_2ZrR^+\cdots A^-$, which is generated when a strong Lewis acid such as $B(C_6F_5)_3$, Ph_3C^+ $B(C_6F_5)_4^-$, or MAO interacts with a zirconocene dialkyl complex.[2]

So far, however, free alkyl zirconocene cations $Cp^x_2ZrR^+$ have been observed only by mass spectrometry in the gas phase.[3] The notion that $Cp^x_2ZrR^+$ cations occur as intermediates in solutions containing ion pairs of the type $Cp^x_2ZrR^+\cdots A^-$ is based mainly if not exclusively on the postulate that an exchange of the anion A^- from one side of the zirconocene complex to the other, which causes a dynamic symmetrization of the NMR spectra of these ion pairs in hydrocarbon solutions, proceeds by way of a dissociative mechanism.[2a,4] Variations in the activation energies for this anion exchange process have thus been proposed to measure variations in the strengths of cation-anion bonds in the alkyl zirconocene ion pairs considered,[4] since the release of the anion from its coordinative contact with the zirconocene cation would be a prerequisite for such a dissociative anion side exchange to occur.

Several lines of reasoning raise the question, however, whether this notion is indeed correct: Many reactions, where neutral ligands such as phosphines, amines, or ethers displace the anion A^- from an ion pair $Cp^x_2ZrR^+\cdots A^-$, recently studied in our laboratories, have all been found to proceed by associative rather than by dissociative mechanisms.[5] In line with this, recent DFT calculations by Ziegler and co-workers place solvated $Cp^x_2ZrR^+$ and A^- ions at energies which are ca. 160 kJ/mol above those of the contact ion pairs $Cp^x_2ZrR^+\cdots A^-$ in toluene solution,[6,7] i.e., substantially higher than the activation energies of 80−100 kJ/mol reported for anion side exchange reactions.[4]

These considerations have lead us to reinvestigate the reaction paths for the dynamic symmetrization of these ion pairs. Here we report results of kinetic studies by 2D-NMR methods on anion exchange dynamics in a series of *ansa*-zirconocene contact ion pairs, generated from the ring-bridged zirconocene dimethyl complexes $Me_4C_2(C_5H_4)_2ZrMe_2$ (**1**), $Me_2Si(C_5H_4)_2ZrMe_2$ (**2**), *rac*-$Me_2Si(Ind)_2ZrMe_2$ (**3**), *rac*-Me_2Si(2-Me-Ind)$_2ZrMe_2$ (**4**), *rac*-Me_2Si(2-Me-Benz[*e*]Ind)$_2ZrMe_2$ (**5**), and *rac*-Me_2Si(2-Me-4-^{t}Bu-$C_5H_4)_2ZrMe_2$ (**6**), which cast substantial doubt on the notion that anion-free, solvated alkyl zirconocene cations are relevant intermediates in these reaction systems.

Results and Discussion

1. Exchange Mechanisms in *ansa*-Zirconocene Ion Pairs. The zirconocene contact ion pairs **1A**−**6A** were generated in situ by reaction of about 1.1 equiv[8] of $B(C_6F_5)_3$[2b] with the respective dimethyl complexes **1**−**6** in C_6D_6 solutions at

(1) Review: Jordan, R. F. *Adv. Organomet. Chem.* **1991,** *32,* 325. Bochmann, M. *J. Chem. Soc., Dalton Trans.* **1996**, 255.

(2) (a) Review: Chen, E. Y.-X.; Marks, T. J. *Chem. Rev.* **2000**, *100*, 1391. (b) Yang, X.; Stern, C. L.; Marks, T. J. *J. Am. Chem. Soc.* **1994**, *116*, 10015. Ewen, J. A.; Elder, M. J. Eur. Patent Appl. 0,427,697, 1991; U.S. Patent 5,561,092, 1996. (c) Chien, J. C. W.; Tsai, W.-M.; Rausch, M. D. *J. Am. Chem. Soc.* **1991**, *113*, 8570. Ewen, J. A.; Elder, M. J. Eur. Patent Appl. 0,426,637, 1991.

(3) Richardson, D. E.; Alameddin, G. N.; Ryan, M. F.; Hayes, T.; Eyler, J. R.; Siedle, A. R. *J. Am. Chem. Soc.* **1996**, *118*, 11244. Feichtinger, D.; Plattner, D. A.; Chen, P. *J. Am. Chem. Soc.* **1998**, *120*, 7125.

(4) (a) Deck, P. A.; Marks, T. J. *J. Am. Chem. Soc.* **1995**, *117*, 6128. Deck, P. A.; Beswick, C. L.; Marks, T. J. *J. Am. Chem. Soc.* **1998**, *120*, 1772. (b) Siedle, A. R.; Newmark, R. A. *J. Organomet. Chem.* **1995**, *497*, 119. Siedle, A. R.; Hanggi, B.; Newmark, R. A.; Mann, K. R.; Wilson, T. *Macromol. Chem. Symp.* **1995**, *89*, 299.

(5) Beck, S.; Prosenc, M. H.; Brintzinger, H. H. *J. Mol. Catal. A: Chem.* **1998**, *128*, 41. Schaper, F.; Brintzinger, H. H. Unpublished results.

(6) Kumar Vanka; Chan, M. S. W.; Pye, C. C.; Ziegler, T. *Organometallics* **2000**, *19*, 1841.

(7) Somewhat lower energies have been calculated for species in which a toluene molecule is coordinated to the Zr center of a $Cp^x_2ZrMe^+$ cation (ref 6). To which degree a species of this type might contribute to anion side exchange would depend, however, on the activation energy and on the stereospecificity of its formation from and reconversion to the respective contact ion pair.

10.1021/ja003531w CCC: $20.00
Published on Web 01/30/2001

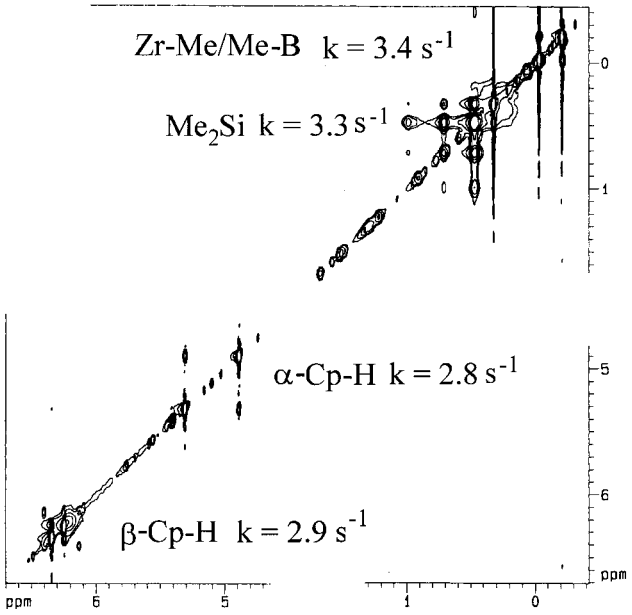

Figure 1. 2D-NOESY spectrum of a solution containing $Me_2Si(C_5H_4)_2$-$ZrMe_2$ and $B(C_6F_5)_3$ in a ratio of 1:1.1 at a zirconocene concentration [Zr] of 19 mmol/L, $T = 303$ K and $\tau_m = 0.1$ s.

Scheme 1

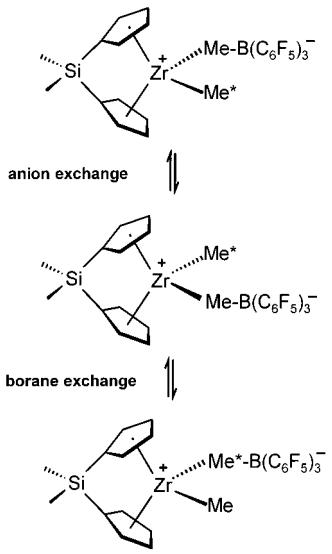

zirconocene concentrations of [Zr] = 10 mmol/L and $T = 300$ K. In their ^{1}H NMR spectra, separate signals are observed for the previously homotopic protons on both sides of the *ansa*-zirconocene ligand framework (Scheme 1). Exchange between these proton sites was monitored in the temperature regime of slow exchange by 2D-NOESY NMR methods. Apparent rate constants were calculated from intensity ratios r of diagonal and cross signals for pairs of previously homotopic protons (cf. Figure 1) according to the equation $k_{app} = (1/\tau_m) \ln[(r + 1)/(r - 1)]$, where τ_m is the mixing time employed and $r = \sum I(\text{diag})/\sum I(\text{cross})$.[9]

For zirconocene contact ion pairs containing the anion Me-$B(C_6F_5)_3^-$, exchange signals between protons on either side of the ligand framework arise either from anion exchange, i.e., side change of the entire anion, or from borane exchange, i.e., exchange of the borane between both Zr-Me groups (Scheme 1).[2a] Exchange signals between terminal and bridging Zr-CH_3 groups, however, can arise only from borane exchange. For complexes **1A**, **3A**, and **4A**, it was not possible to distinguish between these two processes, since their Zr-Me and Zr···μ-Me-B ^{1}H NMR signals were not sufficiently resolved. For complex **2A**, however, the rate of borane exchange was easily measurable and found to be practically equal to the rate with which protons on either side of the *ansa*-zirconocene ligand framework are dynamically symmetrized (Table 1). In this case, anion exchange does not appear to contribute significantly to the exchange between ligand protons. For complexes **5A** and **6A**, on the other hand, cross signals due to borane exchange were not detectable at all at 300 K, even at increased mixing times of $\tau_m = 500$ ms. In these two cases, anion exchange appears to be the dominating process. Complexes **5A** and **6A** show, interestingly, quite different exchange rates, **5A** being the contact ion pair with the slowest and **6A** that with the fastest side exchange.

To corroborate these mechanistic assignments, exchange rates between pairs of ligand proton sites were investigated, again at [Zr] = 10 mmol/L and $T = 300$ K, for the $B(C_6F_5)_3$ adducts **1A**−**6A** at [B]/[Zr] ratios increasing from 1.1:1 to 3:1. The apparent first-order rate constants k_{app} thus obtained (Figure 2) clearly indicate a direct participation of free $B(C_6F_5)_3$ in the exchange process for complexes **1A**−**3A**, presumably by attack of free borane at the terminal Zr-Me group. Ligand side exchange in complexes **4A**−**6A**, on the other hand, appears to be entirely unaffected by excess borane. No exchange signals between terminal and bridging methyl groups are apparent for these complexes either, even in the presence of a 3-fold borane excess.

These results are in line with the observation that borane exchange is the dominant process for complex **2A** but insignificant for **5A** and **6A**; they imply that also complexes **1A** and

Table 1. Apparent First-Order Rate Constants k_{App} (s^{-1}) for Anion Exchange Reactions of Me-$B(C_6F_5)_3^-$-Containing Ion-Pairs **1A**−**6A**,[a] Determined from EXSY Signals in C_6D_6 Solution at 300 K

			k_{app}		
complex[a]	[Zr], mmol/L	[LiMeB-$(C_6F_5)_3$], mmol/L	ligand sides[b]	ZrMe/MeB[c]	Zr-MeB/Li-MeB[d]
1A	4		1.2 ± 0.1	−[e]	
1A	11.7		2.9 ± 0.1	−[e]	
1A	19		3.5 ± 0.1	−[e]	
1A	4	4	2.8 ± 0.1	−[e]	7.3 ± 0.3
2A	4		0.8 ± 0.2	0.7 ± 0.1	
2A	11.7		1.6 ± 0.2	1.6 ± 0.2	
2A	19		3.3 ± 0.2	3.2 ± 0.2	
2A	4	4	2.0 ± 0.1	0.9 ± 0.1	7.2 ± 0.3
3A	4		0.6 ± 0.1	−[e]	
3A	11.7		1.7 ± 0.2	−[e]	
3A	19		2.4 ± 0.5	−[e]	
4A	3		0.36 ± 0.05	−[e]	
4A	5		0.44 ± 0.05	−[e]	
4A	10		0.75 ± 0.1	−[e]	
4A	4	4	0.7 ± 0.05	−[e]	5.2 ± 0.2
5A	2		0.3 ± 0.05	0	
5A	3.5		0.36 ± 0.05	0	
5A	4.8		0.42 ± 0.05	0	
5A	4	4	0.4 ± 0.05	0	0.8 ± 0.05
6A	5		30 ± 1	0	
6A	10		40 ± 1.3	0	
6A	20		52 ± 1.2	0	
6A	4	4	41 ± 2	0	65 ± 1

[a] Generated in situ by reaction of the corresponding zirconocene dimethyl complex with 1.1 equiv of $B(C_6F_5)_3$. [b] For equivalent protons on either side of the ligand framework. [c] For the terminal and bridging Me groups. [d] For Zr-bound and "free" $MeB(C_6F_5)_3^-$. [e] Not sufficiently resolved.

(8) A slight excess of borane was chosen to avoid formation of binuclear cations.

(9) Perrin, C. L.; Dwyer, T. J. *Chem. Rev.* **1990**, *90*, 935.

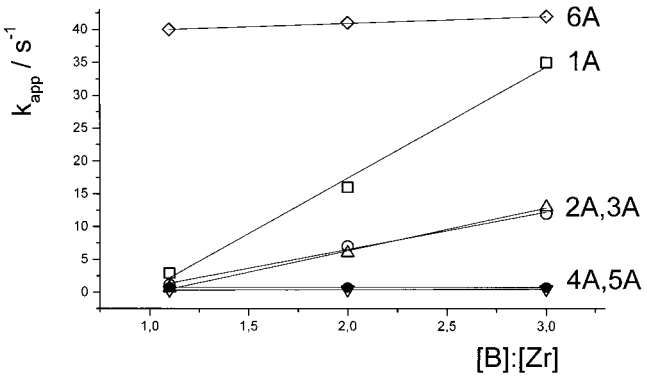

Figure 2. Ligand side exchange rate constants k_{app} (in s^{-1}) for complexes **1A**−**6A** at different [B]/[Zr] ratios (T = 300 K, [Zr] = 10 mmol/L).

3A, like **2A**, undergo dynamic symmetrization predominantly by way of borane exchange, while **4A** is dynamically symmetrized, like **5A** and **6A**, predominantly by anion exchange.

2. Exchange between Contact Ion Pairs 1A−6A and "Free" Me-B(C_6F_5)$_3^-$. To probe the mechanisms of this anion exchange, it would be desirable to determine the effects of excess Me-B(C_6F_5)$_3^-$ anion on the rates of these exchange reactions. "Free" Me-B(C_6F_5)$_3^-$ anions cannot be maintained in any significant concentration in a nonpolar solvent such as C_6D_6, however, as they will be associated here with their countercations. The ^{1}H NMR shift of a Me-B(C_6F_5)$_3^-$ anion can be regarded as a measure of its "freedom": In contact ion pairs with a strong μ-Me coordination, e.g., in (C_5H_5)$_2$ZrMe$^+$···μ-Me-B(C_6F_5)$_3^-$, its ^{1}H NMR signal appears at ca. 0.1 ppm; ^{1}H NMR signals at ca. 1.3−1.4 ppm are found, on the other hand, in "outer-sphere" ion pairs with (C_5H_5)$_2$ZrMe(PMe$_3$)$^+$ countercations, which are likely to be associated only with the aromatic residues of the Me-B(C_6F_5)$_3^-$ anion.[2a,5] This countercation is not sufficiently inert, however, and tends to undergo side reactions with some of the contact ion pairs considered here. For this reason we have chosen the ion pair Li$^+$··· Me-B(C_6F_5)$_3^-$, which gives rise to an ^{1}H NMR signal with an intermediate shift of ca. 0.8 ppm, as a source of "free" Me-B(C_6F_5)$_3^-$ anions.

Addition of 1 equiv of Li$^+$···Me-B(C_6F_5)$_3^-$ to C_6D_6 solutions of contact ion pairs **1A**−**6A** gave the rate changes summarized in Table 1: For complexes **1A** and **2A,** a 2−3-fold increase in the rate of ligand proton side exchange was induced by Li$^+$···Me-B(C_6F_5)$_3^-$, while borane exchange was found to continue at about the same rate.

In addition, it was found that Li$^+$···Me-B(C_6F_5)$_3^-$ exchanges with the Zr-bound Me-B(C_6F_5)$_3^-$ anions of complexes **1A** and **2A** at a rate that is about 3-fold greater than that of the side exchange occurring in the respective contact ion pair by itself (Table 1). Apparently, associative attack of Me-B(C_6F_5)$_3^-$ at a Zr center occurs rather frequently under these conditions, but predominantly in an unproductive manner, i.e., at the Zr-anion side of the contact ion pair, and only occasionally so that attack from the ZrMe side results in side exchange.

That contact ion pairs such as **2A** are now susceptible to anion exchange, to which they were inert by themselves, might be due to the presence of the Lewis-acidic Li$^+$ cation,[10] which could either increase electrophilicity at the Zr center by interaction with the terminal Zr-Me group or — in the case of nonproductive anion-anion exchange — direct the incoming anion into the vicinity of the leaving anion by coordinating both of these entities.

(10) Staley, R. H.; Beauchamp, J. L. *J. Am. Chem. Soc.* **1975**, *97*, 5920.

Scheme 2

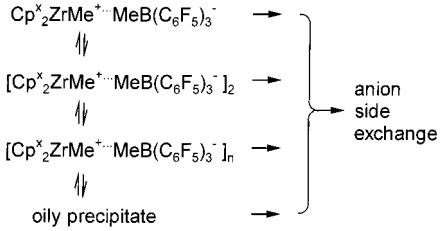

In complexes **4A**, **5A**, and **6A** anion exchange is accelerated by addition of Li$^+$···Me-B(C_6F_5)$_3^-$ by factors of 1.2−1.5 (Table 1). These rather congested complexes thus appear to be more resilient to associative attack by Me-B(C_6F_5)$_3^-$. Even for these complexes, however, the rates of exchange between "free" and Zr-bound Me-B(C_6F_5)$_3^-$ anions are almost twice as high as their side exchange rates, indicating again substantial nonproductive anion exchange.

3. Effects of Zirconocene Concentrations on Side Exchange Rates. To clarify whether the exchange reactions considered proceed unimolecularly, as had been assumed so far,[4] we have determined the dependence of exchange rates on zirconocene concentrations and, in doing so, made the unexpected observation that these side exchange rates are significantly dependent on zirconocene concentrations for all contact ion pairs studied.

Depending on their solubilities, the B(C_6F_5)$_3$ adducts **1A**−**6A** were investigated at zirconocene concentrations in the range of [Zr] = 2−20 mmol/L. All solutions were measured at T = 300 K and at a [B]/[Zr] ratio of 1.1:1. The apparent pseudo-first-order rate constants k_{app} for the side-exchange reaction, derived from 2D-NOESY data (Table 1), clearly increase with increasing Zr concentrations. Plots of ln(k_{app}) versus ln([Zr]) reveal broken reaction orders of n = 1.4−1.8 with regard to Zr concentrations, with exponents n rather close to 2 (n = 1.7−1.8) for systems **1A**−**3A**, while somewhat smaller values (n = 1.3−1.4) pertain for systems **4A**−**6A**.

For an interpretation of these fractional reaction orders one has to take into account that ion quadruples (and probably also more highly aggregated species) are present in concentration-dependent equilibria with the monodispersed contact ion pairs at the zirconocene concentrations considered here (Scheme 2).[11,12] If these ion quadruples have higher intrinsic exchange rates than the monomeric ion pairs, the observed rates would be expected to increase with [Zr]^2 at low zirconocene concentrations, but would approach proportionality to [Zr] as ion quadruples become the dominant species in the monomer−dimer equilibrium. The observed fractional reaction order with regard to [Zr] would thus be compatible with the view that anion exchange occurs predominantly in dimeric (or higher) aggregates of the contact ion pairs considered.

In a polynuclear species, intermolecular interactions between ion pairs will certainly be facilitated. The anion exchange occurring in dimers of the ion pairs **4A**−**6A** can be envisioned to proceed by way of intermolecular Zr$^+$-fluoroaryl interactions, for which substantial precedence has been reported.[13] Anion exchange via a transition state of the type represented in Scheme 3 would first yield F-coordinated contact ion pairs, which can

(11) Beck, S.; Geyer, A.; Brintzinger, H. H. *Chem. Commun.* **1999**, 2477.

(12) Changes in ionic strength of these solutions, which might be argued to affect the observed exchange rates, are tantamount to changes in the degree of aggregation. Keeping ionic strengths constant by addition of "inert" salts is likely to cause added complexity due to formation of mixed ion aggregates in these solutions.

(13) Horton, A. D.; Orpen, A. G. *Organometallics* **1991**, *10*, 3910. Yang, X.; Stern, C. L.; Marks, T. J. *Organometallics* **1991**, *10*, 840.

Scheme 3

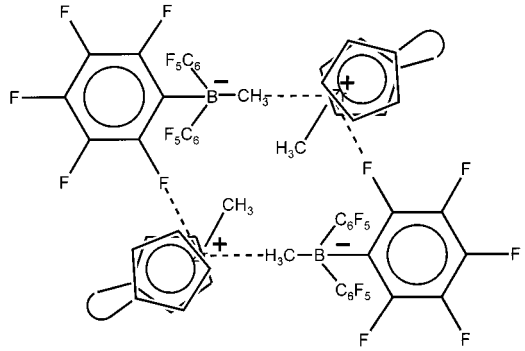

Table 2. Activation Parameters for Side Exchange of the Me-$B(C_6F_5)_3^-$-Containing Ion-Pairs **1A**−**6A** and of the $B(C_6F_5)_4^-$-Containing Ion-Pairs **1B**−**3B** and **5B**, Determined from Apparent First-Order Rate Constants Measured at 300, 305, and 310 K in d_6-Benzene Solution, and at 252, 257, and 260 K in d_8-Toluene Solution, Respectively.

complex	[Zr] mmol/L	$\Delta H^{\ddagger}$, kJ/mol	$\Delta S^{\ddagger}$, J/(mol·K)
1A	10	50 ± 4	−76 ± 1
2A	10	48 ± 2	−81 ± 8
3A	10	40 ± 8	−108 ± 10
4A	10	53 ± 9	−40 ± 3
5A	5	81 ± 4	17 ± 4
6A	5	58 ± 4	−48 ± 5
6A	10	62 ± 3	−9 ± 5
1B	1	57 ± 3	8 ± 8
2B	1	50 ± 8	−30 ± 20
3B	1	67 ± 8	27 ± 15
5B	1	85 ± 9	102 ± 25

then isomerize to a methyl-borate coordinated geometry by an intramolecular, presumably facile rearrangement. Even though such a process would be formally unimolecular with respect to the ion quadruple, it would be of the associative type since the coordination number of the Zr center is increased in the exchange transition state.

4. Temperature Dependence of Exchange Rates. Activation parameters for these side-exchange reactions were determined by measuring their rates at temperatures of T = 300, 305, 310, and 315 K in C_6D_6 solutions at a [B]/[Zr] ratio of 1.1:1 and by analyzing Eyring plots for the apparent first-order rate constants k_{app} (Table 2).[14]

While activation entropies for these broken-order reactions are to be interpreted with caution, the effect of changing zirconocene concentrations, which was determined for complex **6A**, is quite illuminating: $\Delta H^{\ddagger}$ is practically unaffected by a concentration change; $\Delta S^{\ddagger}$ values, however, are more positive by ca. 35−40 J/(mol·K) at [Zr] = 10 mmol/L than at [Zr] = 5 mmol/L.[14] The data given in Table 2 indicate that the accelerating effect of increased zirconocene concentrations originates solely from less unfavorable entropy changes along the reaction coordinate. This is in line with the notion that more highly aggregated species, such as ion quadruples, are involved in these exchange reactions: Anion-exchange transition states such as that represented in Scheme 3 can obviously be reached from a preformed ion quadruple with very little further preordering.

5. Dynamics of *ansa*-Zirconocene Ion Pairs with $B(C_6F_5)_4^-$ Anions. Ion pairs **1B**−**3B** and **5B**, generated from the corresponding dimethyl complexes by reaction with $Ph_3C^+ B(C_6F_5)_4^-$,[2c] rather than with $B(C_6F_5)_3$, undergo ligand side exchange, under otherwise comparable conditions ([Zr] = 1.0 mmol/L; [B]/[Zr]= 1.1:1), about 5000 times faster than the corresponding Me-$B(C_6F_5)_3^-$ ion pairs, i.e., too fast for 2D-NMR measurements at room temperature. Measurements at temperatures of T = 252, 257, and 260 K in d_8-toluene solutions gave, from Eyring plots of the apparent first-order rate constants k_{app}, the $\Delta H^{\ddagger}$ and $\Delta S^{\ddagger}$ values listed in Table 2.

Remarkably, we find $\Delta H^{\ddagger}$ values for complexes **1B**−**3B** and **5B** which are close to those found above for the respective ion pairs with Me-$B(C_6F_5)_3^-$ anions. Enthalpic contributions, i.e., a reduced strength of the cation−anion bond, are thus apparently not the cause for the higher rates of exchange in $B(C_6F_5)_4^-$ ion pairs. $\Delta S^{\ddagger}$ values, however, are more positive by ca. 50−100 J/(mol·K) for these complexes than for the corresponding species with Me-$B(C_6F_5)_3^-$ anions.[14]

These observations are strikingly similar to those associated with a concentration increase of the Me-$B(C_6F_5)_3^-$ -containing ion pairs and lead us to propose that the $B(C_6F_5)_4^-$ -containing ion pairs **1B**−**3B** and **5B** behave as their Me-$B(C_6F_5)_3^-$ -containing analogues would if their concentrations were even higher than those used here. Apparently, the more polar ion pairs **1B**−**3B** and **5B** form increased proportions of rapidly exchanging ion quadruples or higher aggregates already at relatively low concentrations in the nonpolar solvent used. This notion is supported by the observation that the $B(C_6F_5)_4^-$ -containing ion pairs tend to form a separate oily phase already at concentrations which are about an order of magnitude lower than those at which their Me-$B(C_6F_5)_3^-$ -containing analogues begin to separate from their hydrocarbon solutions. These observations indicate that even a particularly weakly coordinating anion such as $B(C_6F_5)_4^-$ might exchange predominantly by an associative mechanism.

6. Crystal Structure of *rac*-$Me_2Si(2\text{-}Me\text{-}4\text{-}^tBu\text{-}C_5H_2)_2Zr\text{-}Me^+\cdots\mu\text{-}MeB(C_6F_5)_3^-$. Whereas a number of crystal structures have been reported for ion pairs of the type $Cp^*_2ZrMe^+\cdots\mu$-Me-$B(C_6F_5)_3^-$,[2a,15,16] chiral representatives of this class of complexes have not been structurally characterized so far. Attempts to obtain crystals of ion pairs of the racemic complexes **3**, **4**, and **5** failed due to the formation of oily precipitates. The $B(C_6F_5)_3$ adduct of *rac*-$Me_2Si(2\text{-}Me\text{-}4\text{-}^tBu\text{-}C_5H_2)_2ZrMe_2$, however, was isolated in the form of single crystals. Although the crystals and the resulting X-ray diffraction data were not of particularly high quality, the essential bond lengths and bond angles of complex **6A** lie within the range of values reported before for other μ-Me$B(C_6F_5)_3^-$ contact ion pairs (Figure 3, Table 3).[2a,15,16]

Table 3. Selected Bond Distances (pm) and Angles (deg) for Complex **6A** and Two Related Contact Ion Pairs

	1A[a]	**6A**	**7A**[b]
Zr-μ-CH_3	251.6(8)	255.0(8)	254.9(3)
H_3C-μ-B	167.8(12)	168.8(13)	166.3(5)
Zr-CH_3	225.8(9)	229.4(8)	225.2(4)
Zr-μ-CH_3-B	171.5(5)	162.7(6)	161.8(2)
C-Zr-μ-CH_3	91.8(3)	92.1(4)	92.0(1)

[a] From ref 16. [b] $(1,2\text{-}Me_2C_5H_3)_2ZrMe\text{-}\mu\text{-}MeB(C_6F_5)_3$, from ref 4a.

A crystal-packing representation of complex **6A** shows the aggregation of contact ion pairs to rhombus-shaped ion quadruples (Figure 4, left). In a packing representation of the

(14) Eyring-plot analysis of second-order rate constants k_{sec}, derived from k_{app} by division through [Zr], has no effect on the values of $\Delta H^{\ddagger}$ and gives $\Delta S^{\ddagger}$ values which are more positive than those obtained from k_{app} by about 40 J/(mol·K) throughout. This does not affect the comparison of $\Delta S^{\ddagger}$ values at different zirconocene concentrations or of contact ion pairs with $B(C_6F_5)_4^-$ and with Me-$B(C_6F_5)_3^-$ anions.

(15) Bochmann, M.; Lancaster, S. J.; Hursthouse, M. B.; Malik, K. M. A. *Organometallics* **1994**, *13*, 2235.

(16) Beck, S.; Prosenc, M. H.; Brintzinger, H. H.; Goretzki, R.; Herfert, N.; Fink, G. *J. Mol. Catal. A: Chem.* **1996**, *111*, 67.

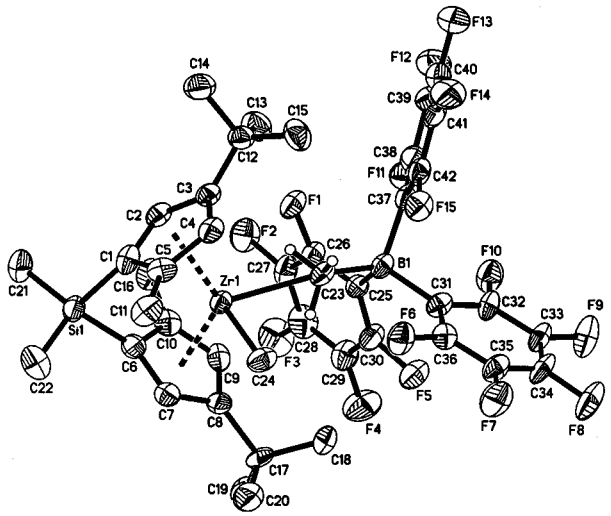

Figure 3. ORTEP/PLUTO drawing of the molecular structure of the contact ion pair *rac*-$Me_2Si(2\text{-}Me\text{-}4\text{-}^tBu\text{-}C_2H_2)_2ZrMe^+\cdots\mu\text{-}MeB(C_6F_5)_3^-$ (**6A**). H atoms were omitted for clarity.

previously determined crystal structure of complex **1A**,[16] aggregation of contact ion pairs to ion quadruples is similarly evident (Figure 4, right). Several relatively short intermolecular Zr−F distances of ca. 450−550 pm indicate dipolar interactions of C−F units with a cationic Zr center.

Solid-state structures such as those of **1A** or **6A** are a priori likely to contain rhombi of their constituent ions and should thus not be overinterpreted with respect to possible interactions in solution. Nonetheless, they illustrate possible proximity relations in an ion quadruple and let it appear plausible that anion-exchange transition states similar to that represented in Scheme 3 might be accessible from ion-quadruples without much further preordering.

Conclusions

The weight of the evidence described above — in particular the acceleration of the dynamic symmetrization of zirconocene ion pairs by added $Li^+\cdots Me\text{-}B(C_6F_5)_3^-$, the nonproductive anion exchange which accompanies this rate increase, the increase of exchange rates with increasing concentrations of the zirconocene ion pairs, and, finally, the exclusively entropic nature of these concentration-dependent rate changes — indicates that anion exchange in nonpolar solutions of these ion pairs proceeds predominantly by way of ion quadruples or higher order ionic aggregates. As long as there is no conclusive evidence that this anion exchange occurs — at least in parts — by way of dissociative, unimolecular reaction paths, it should be seriously questioned whether solvated zirconocene alkyl cations of the type $Cp^x_2ZrMe^+$ are capable of existing, free of a supporting ligand, even as short-lived reaction intermediates in reaction systems containing $Cp^x_2ZrMe^+\cdots A^-$ ion pairs in hydrocarbon solutions.[17]

If anion-free $Cp^x_2Zr(alkyl)^+$ cations are indeed unavailable as intermediates in these reaction systems, their implication as active species of zirconocene-based catalysts for the polymerization of α-olefins would appear inappropriate. Instead, substitution reactions in which the anion is displaced from these ion pairs by nucleophilic attack of an olefin substrate (or a competing entity) would have to be studied with regard to their thermodynamics and kinetics to establish useful structure-

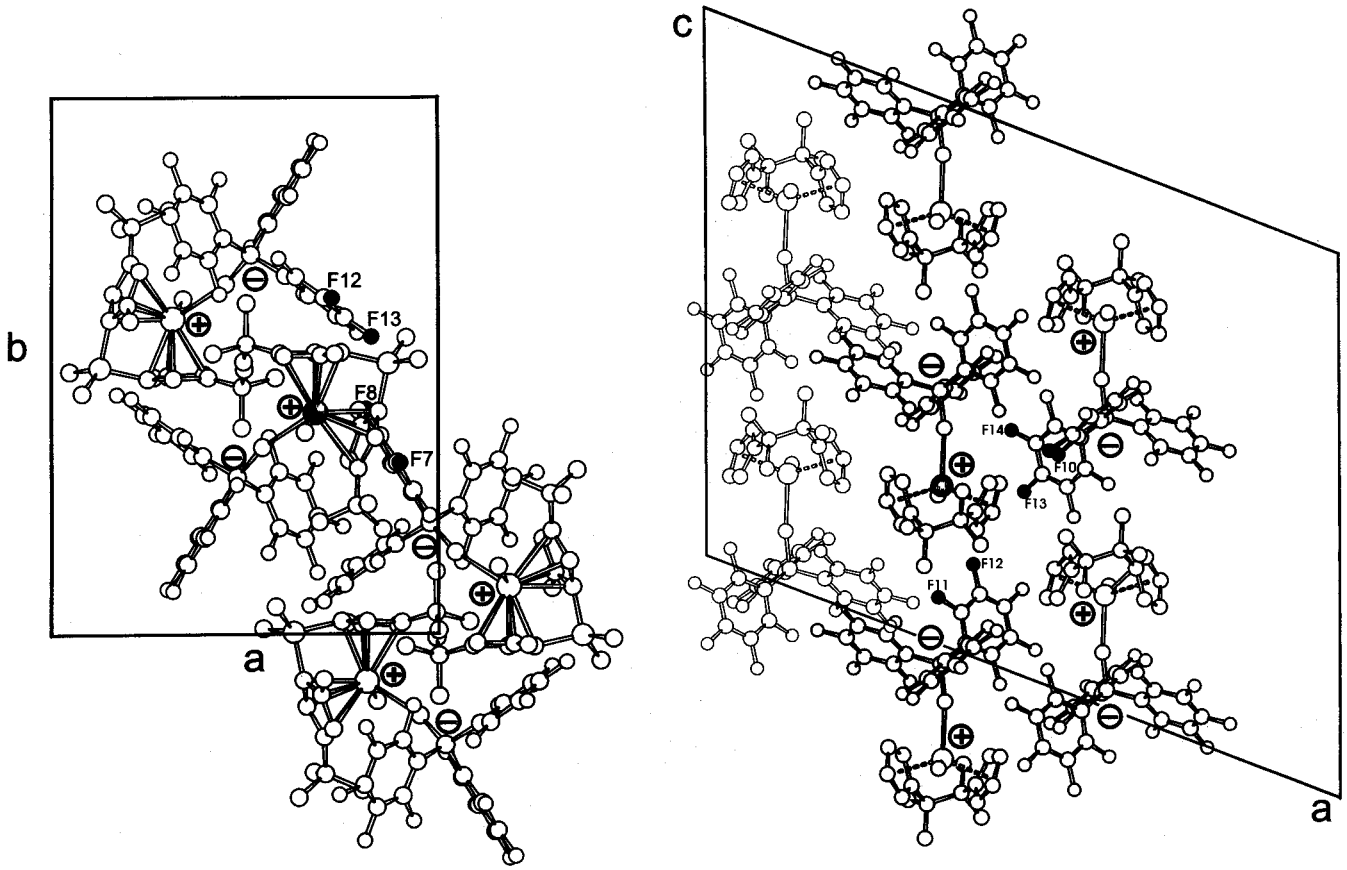

Figure 4. Schakal drawings of the crystal packing of complexes **6A** (left) and **1A** [16] (right), projected along the unit-cell *c* and *b* axes, respectively. Black F atoms are within less than 600 pm from the shaded Zr centers. Circled plus and minus signs indicate the approximate location of cationic and anionic charges, respectively.

property relations for metallocene-based polymerization catalysts.

Experimental Section

All reactions were performed under argon with Schlenk-line techniques or under nitrogen in a glovebox. Solvents were dried prior to use by refluxing over and distillation from sodium. Deuterated solvents were dried over 4 Å molecular sieves. Zirconocene dimethyl complexes (**1**−**5**) were synthesized according to ref 18, $B(C_6F_5)_3$ according to ref 19. $[Ph_3C][B(C_6F_5)_4]$ was obtained as a gift from BASF AG, $Me_2Si(2\text{-Me-ind})_2ZrCl_2$ from Axiva GmbH. Other chemicals were purchased from commercial suppliers and used without further purification. Exchange NMR spectra were recorded on a Bruker Avance DRX 600 (600 MHz) instrument.

***rac*-$Me_2Si(2\text{-Me-Ind})_2ZrMe_2$ (4).** In 80 mL of toluene, 476 mg (1 mmol) of *rac*-$Me_2Si(2\text{-Me-Ind})_2ZrCl_2$ was dissolved in a double Schlenk vessel and cooled to −15 °C. After addition of 2.1 equiv of a solution of MeMgCl in ether the mixture was allowed to warm to room temperature and stirred overnight, while the color turned from orange to light yellow and a white solid precipitated. The solvent was removed in vacuo and the residue extracted three times with toluene. Crystallization from pentane at −80 °C afforded yellow needles in 70% yield.

^{1}H NMR (250 MHz, C_6D_6, 7.15 ppm, 300 K) δ 7.16 (d, 2H, Ind-7), 6.77 (t, 2H, Ind-6), 7.39 (t, 2H, Ind-5), 7.42 (d, 2H, Ind-4), 6.59 (s, 2H, Ind-3), 1.89 (s, 6H, 2-Me), 0.73 (s, 6H, Me_2Si), −0.87 (s, 6H, Zr-Me).^{13}C NMR (150 MHz; C_6D_6, 128 ppm; 300 K) δ 134.4, 129.7 (Ind-3a, Ind-7a), 125.8 (Ind-4), 125.7 (Ind-5), 124.5 (Ind-7), 123.6 (Ind-6), 115.8 (Ind-3), 79.0 (Ind-1), 36.1 (Zr-Me), 18.0 (2-Me), 2.4 (Me_2-Si).

***rac*-$Me_2Si(2\text{-Me-4-}^t\text{Bu-}C_5H_2)_2ZrMe_2$ (6).** To a solution of 245 mg (0.5 mmol) of *rac*-$Me_2Si(2\text{-Me-4-}^t\text{Bu-}C_5H_2)_2ZrCl_2$ in ether at 0 °C was added, under exclusion of light, 1.2 mL (1.2 mmol) of a 1 M solution of MeMgCl in ether. After stirring the reaction mixture overnight and removal of the solvent by evaporation, the residue was extracted three times with pentane. Concentration of the solution to about half of its volume in vacuo and cooling to −80 °C afforded complex **6** in the form of white needles. Yield 120 mg (55%). ^{1}H NMR (250 MHz, C_6D_6, 300 K) δ 0.88 (bs, 3H, B-Me), 6.44 (d, 2H, (C_5H_2)), 5.33 (d, 2H, (C_5H_2)), 1.85 (s, 6H, (2-CH_3)), 1.37 (s, 18H, (4-C(CH_3)$_3$)), 0.34 (s, 6H, (CH_3)$_2$Si), 0.14 (s, 6H, $ZrCH_3$). Anal. Found: C, 64.3; H, 9.3. Calcd: C, 64.4; H, 9.0.

Li^+ $MeB(C_6F_5)_3^-$. In a glovebox, 1.1 mg (50 μmol) of solid MeLi, dried by evaporation of an etheral solution and coevaporation with pentane, were mixed with 28.5 mg (55 μmol) of tris(pentafluorophenyl)-borane dissolved in 2.3 mL of benzene. The mixture was stirred for 1 h until a clear solution was obtained. **Caution**: A 100-mg sample of dry $LiMeB(C_6F_5)_3$ underwent detonation upon contact with a spatula. $LiMeB(C_6F_5)_3$ should thus be prepared in small portions only and its solutions should not be allowed to evaporate to dryness.

NMR Measurements. All exchange reactions were monitored by NOESY experiments, using mixing times τ_m = 50−500 ms, which were chosen so as to obtain a diagonal-to-cross signal ratio of about 4/1. Apparent first-order rate constants k_{app} were evaluated from the signal intensities of at least two different proton positions of the molecule studied and calculated according to the equation $k_{app} = (1/\tau_m)\ln[(r+1)/(r-1)]$ with $r = \sum I(\text{diag})/\sum I(\text{cross})$.[9]

Solutions of the zirconocene ion pairs were prepared by transferring, with an Eppendorf pipet, stock solutions containing the zirconocene dimethyl complexes **1**−**4** and **6** at zirconocene concentrations [Zr] = 40 mmol/L and complex **5** at [Zr] = 10 mmol/L and solutions containing the activator components, $B(C_6F_5)_3$ at c = 40 mmol/L and $Ph_3C^+B(C_6F_5)_4^-$ at c = 5 mmol/L, directly to an NMR tube in the glovebox. The NMR tubes were stoppered and immediately transferred to the spectrometer.

$Me_4C_2(C_5H_4)_2ZrMe^+$-μ-Me-$B(C_6F_5)_3^-$ (1A). ^{1}H NMR (600.1 MHz, C_6D_6, 7.15 ppm, 300 K) δ 6.09 (pq, 2H, β-Cp, Zr-Me-side), 5.89 (pq, 2H, β-Cp, Me-B-side), 5.58 (pq, 2H, α-Cp, Me-B-side), 5.05 (pq, 2H, α-Cp, Zr-Me-side), 0.74 (s, 6H, Me_4C_2, Me-B-side), 0.59 (s, 6H, Me_4C_2, Zr-Me-side), 0.38 (s, 3H, Zr-Me), 0.32 (br, 3H, Me-B).

Exchange rates were determined from α-Cp-H, β-Cp, and Me_4C_2 signals (mixing times τ_m given in parentheses): T = 300 K, [Zr]:[B] = 1:1.1; [Zr] = 3.95, 11.65, and 19.05 mM (200 ms); T = 300K, [Zr] = 10 mM, [Zr]:[B] = 1:1.1, 2, and 3 (50 ms); T = 300, 305, 310, and 315 K, [Zr]= 10 mM, [Zr]:[B] = 1:1.1 (200 ms).

$Me_2Si(C_5H_4)_2ZrMe^+$-μ-Me-$B(C_6F_5)_3^-$ (2A). ^{1}H NMR (600.1 MHz, C_6D_6, 7.15 ppm, 300 K) δ 6.34 (pq, 2H, β-Cp Zr-Me-side), 6.24 (pq, 2H, β-Cp Me-B-side), 5.30 (pq, 2H,α-Cp Me-B-side), 4.89 (pq, 2H, α-Cp Zr-Me-side), 0.47 (br, 3H, Me-B), 0.32 (s, 3H, Zr-Me), −0.03 (s, 3H, Me_2Si Me-B-side), −0.21 (s, 3H, Me_2Si Zr-Me-side).

Exchange rate constants were determined for the α-Cp, β-Cp, and Me_2Si signals (mixing times τ_m given in parentheses): T = 300 K, [Zr]:[B] = 1:1.1, [Zr] = 19.05, 11.65 (100 ms) and 3.95 mM (150ms); T = 300 K, [Zr] = 10 mM, [Zr]:[B] = 1:1.1, 1:2 (150 ms), and 1:3 (100 ms); T = 303, 308, 313, and 318 K, [Zr] = 10 mM, [Zr]:[B] = 1:1.1 (150 ms).

***rac*-$Me_2Si(Ind)_2ZrMe^+$-μ-Me-$B(C_6F_5)_3^-$ (3A).** ^{1}H NMR (600.1 MHz, C_6D_6, 7.15 ppm, 300 K) δ 7.50 (d, 1H, Ind-H), 7.03 (m, 2H, Ind-H), 6.89 (d, 1H, Ind-H), 6.69 (m, 1H, Ind-H), 6.63 (m, 1H, Ind-H), 6.57 (d, 1H, β-C_5H_2 Zr-Me-side), 6.29 (m, 2H, Ind-H), 6.22 (d, 1H, β-C_5H_2 Me-B-side), 5.66 (d, 1H, α-C_5H_2 Me-B-side), 4.97 (d, 1H, α-C_5H_2 Zr-Me-side), 0.34 (s, 3H, Me_2Si), 0.20 (s, 3H, Me_2Si), −0.44 (br, 3H, Me-B), −0.51 (s, 3H, Zr-Me).

Exchange rate constants were determined for the α-C_5H_2 and Me_2-Si signals (mixing times τ_m are given in parentheses): T = 300 K, [Zr]:[B] = 1:1.1, [Zr] = 3.95, 11.65, and 19.05 mM (200 ms); T = 300 K, [Zr] = 10 mM, [Zr]:[B] = 1:1.1, 1:2, and 1:3 (200 ms); [Zr] = 10 mM, [Zr]:[B] = 1:1.1, T = 300 (200 ms), 305 (75ms), 310 (50 ms), and 315 K (25 ms).

***rac*-$Me_2Si(2\text{-Me-Ind})_2ZrMe^+$-$\mu$-Me-$B(C_6F_5)_3^-$ (4A).** ^{1}H NMR (600.1 MHz, C_6D_6, 7.15 ppm, 300 K) δ 6.93 (d, 1H, Ind-7), 6.55 (t, 1H, Ind-6), 7.04 (t, 1H, Ind-5), 7.55 (d, 1H, Ind-4), 7.0 (d, 1H, Ind-7′), 6.36 (d, 1H, Ind-6′), 6,21 (t, 1H, Ind-5′), 7.06 (d, 1H, Ind-4′), 6.12 (s, 1H, C_5H-3′), 6.39 (s, 1H, C_5H-3′), 1.70 (s, 3H, MeC_5H-2), 1.44 (s, 3H, MeC_5H-3′), 0.44 (s, 3H, Me_2Si-1-side), 0.49 (s, 3H, Me_2Si-1′-side), −0.26 (br, 3H, Me-B), −0.29 (s, 3H, Zr-Me).

Exchange rate constants were determined for the α-C_5H and 2-Me signals (mixing times τ_m given in parentheses): T = 300 K, [Zr]:[B] = 1:1.1, [Zr] = 3, 5, and 10 mM (300 ms); T = 300 K, [Zr] = 10 mM, [Zr]:[B] = 1:1.1, 1:2, and 1:3 (300 ms); [Zr] = 10 mM, [Zr]:[B] = 1:1.1, T = 300 (200 ms), 305 (75 ms), 310 (50 ms), and 315 K (25 ms).

***rac*-$Me_2Si(2\text{-Me-Benz}[e]\text{Ind})_2ZrMe^+$-$\mu$-Me-$B(C_6F_5)_3^-$ (5A).** ^{1}H NMR (600.1 MHz, C_6D_6, 7.15 ppm, 300 K) δ 7.86 (d, 1H, Benz-9), 7.68 (d, 1H, Benz-9′), 7.61 (t, 1H, Benz-8), 7.49 (d, 1H, Benz-6), 7.29 (t, 1H, Benz-7), 7.16 (nr, 1H, Benz-6′), 7.12 (1H, Benz-8′), 7.08 (1H, Benz-7′), 7.04 (1H, Ind-5), 6.97 (1H, Ind-4), 6.97 (1H, Ind-1), 6.95 (1H, Ind-5′), 6.74 (1H, Ind-4′), 6.73 (1H, Ind-1), 1.87 (s, 3H, 2-Me), 1.65 (s, 3H, 2-Me′), 0.564 (s, 3H, Me_2Si), 0.558 (s, 3H, Me_2Si), −0.34 (br, 3H, Me-B), −0.41 (s, 3H, Zr-Me).

Exchange rate constants were determined for the H-9,9′ (7.86/7.68 ppm), H-6,6′ (7.49/ 7.16 ppm), and 2-Me signals (mixing times τ_m given in parentheses): T = 300 K, [Zr]:[B] = 1:1.1, [Zr] = 2, 3.6, and 4.76 mM (400 ms); T = 300, 305, 310, and 315 K, [Zr] = 5 mM, [Zr]:[B] = 1:1.1 (400 ms).

***rac*-$Me_2Si(2\text{-Me-4-}^t\text{Bu-}C_5H_2)_2ZrMe^+$-$\mu$-MeB$(C_6F_5)_3^-$ (6A).** ^{1}H NMR (600.1 MHz, C_6D_6, 7.15 ppm, 300 K) δ 6.21, 6.10 (bs, 2, β-C_5H_2); 5.26, 4.96 (bs, 2, α-C_5H_2); 1.69, 1.4 (bs, 6, $CH_3C_5H_2$); 0.96, 0.72 (bs, 18, (CH_3)$_3CC_5H_2$); 0.7 (bs, 3, BCH_3); 0.63 (s, 3, $ZrCH_3$); 0.12 (bs, 3, (CH_3)$_2$Si), −0.03 (bs, 3, (CH_3)$_2$Si).

Exchange rate constants were determined for the α-Cp-H, β-Cp-H, and Me_2Si signals (mixing times τ_m given in parentheses): T = 300 K, [Zr]:[B] = 1:1.1, [Zr] = 5, 10, and 20 mM (10, 15, and 35 ms); T

(17) In halocarbon solvents, higher dielectric constants and action of the halocarbons as stabilizing ligands might favor formation of anion-free alkyl zirconocene cations.

(18) Wiesenfeldt, H.; Reinmuth, A.; Barsties, E.; Evertz, K.; Brintzinger, H. H. *J. Organomet. Chem.* **1989**, *369*, 359.

(19) Pohlmann, J. L. W.; Brinckman, F. E.; Tesi, G.; Donadio, R. E. *Z. Naturforsch.* **1965**, *20b*, 1. Pohlmann, J. L. W.; Brinckman, F. E. *Z. Naturforsch.* **1965**, *20b*, 5.

= 300 K, [Zr] = 10 mM, [Zr]:[B] = 1:1.1, 2, and 3 (15 ms); T = 300, 305, 310, and 315 K, [Zr]= 5, 10 mM, [Zr]:[B] = 1:1.1 (15 and 5 ms).

$[Me_4C_2(C_5H_4)_2ZrMe]^+ B(C_6F_5)_4^-$ (1B). ^{1}H NMR (600.1 MHz, C_7D_8, 2.09 ppm, 252 K) δ 6.10 (br, 2H, β-Cp-H), 5.36 (br, 2H, α-Cp-H), 4.88 (br, 2H, α-Cp-H), 4.88 (br, 2H, β-Cp-H), 0.74 (s, 6H, Me_4C_2), 0.87 (s, 6H, Me_4C_2), 0.26 (s, 3H, Zr-Me), 2.00 (s, 3H, Me-CPh_3).

Exchange rate constants were determined for the α-Cp-H, β-Cp-H ,and Me_4C_2 signals (0.74/0.87 ppm; mixing times τ_m given in parentheses): [Zr]:[B] = 1:1.1, [Zr] = 1 mM, T = 252 (100 ms), 257 (50 ms), and 260 K (10 ms).

$[Me_2Si(C_5H_4)_2ZrMe]^+ B(C_6F_5)_4^-$ (2B). ^{1}H NMR (600.1 MHz, C_7D_8, 2.09 ppm, 252 K) δ 6.30 (br, 2H, β-Cp-H), 5.19 (br, 2H, α-Cp-H), 5.10 (br, 2H, α-Cp-H), 4.66 (br, 2H, β-Cp-H), 0.17 (s, 3H, Me_2Si), −0.17 (s, 3H, Me_2Si), 0.17 (s, 3H, Zr-Me), 2.00 (s, 3H, Me-CPh_3).

Exchange rate constants were determined for the α-Cp-H, β-Cp-H, and Me_2Si signals (0.17/−0.17 ppm; mixing times τ_m given in parentheses): [Zr]:[B] = 1:1.1, [Zr] = 1 mM, T = 252 (150 ms), 257 (100 ms), and 260 K (50 ms).

$[rac\text{-}Me_2Si(Ind)_2ZrMe]^+ B(C_6F_5)_4^-$ (3B). ^{1}H NMR (600.1 MHz, C_7D_8, 2.09 ppm, 252 K) δ 5.19 (d, 2H, α-C_2H_5), 4.85 (d, 2H, α-C_2H_5), 0.47 (s, 3H, Me_2Si), −0.16 (s, 3H, Me_2Si), −0.78 (s, 3H, Zr-Me), 2.00 (s, 3H, Me-CPh_3).

Exchange rate constants were determined for α-C_5H_2 and Me_2Si signals (mixing times τ_m given in parentheses): [Zr]:[B] = 1:1.1; [Zr] = 1 mM; T = 252, 257, and 260 K (100 ms).

$[rac\text{-}Me_2Si(2\text{-}Me\text{-}Benz[e]Ind)_2ZrMe]^+ B(C_6F_5)_4^-$ (5B). ^{1}H NMR (600.1 MHz, C_7D_8, 2.09 ppm, 252 K) δ 1.69 (s, 3H, 2-Me), 1.58 (s, 3H, 2-Me), 0.75 (s, 3H, Me_2Si), 0.53 (s, 3H, Me_2Si), −0.66 (s, 3H, Zr-Me), 2.00 (s, 3H, Me-CPh_3).

Exchange rate constants were determined for 2-Me and Me_2Si signals (mixing times τ_m in parentheses): [Zr]:[B] = 1:1.1, [Zr] = 1 mM, T = 252 (150 ms) and 257 and 260 K (100 ms).

$[rac\text{-}Me_2Si(2\text{-}Me\text{-}4\text{-}^t Bu\text{-}C_5H_2)_2ZrMe]^+ B(C_6F_5)_4^-$ (6B). Exchange rates were too fast, even at 240 K, for separate signals to be observable.

Exchange Rates with Added $Li^+ MeB(C_6F_5)_3^-$. Rate constants were determined for the symmetrization of the ligand framework and for exchange between zirconium-bound $MeB(C_6F_5)_3^-$ and $Li^+MeB(C_6F_5)_3^-$ at [Zr]:[B] = 1:1.1, [Zr] = 4 mM, $[Li^+MeB(C_6F_5)_3^-]$ = 4 mM; T =300 K, mixing times τ_m in parentheses: $Me_4C_2(C_5H_4)_2ZrMe^+$-μ-Me-$B(C_6F_5)_3^-$ (250 ms); $Me_2Si(C_5H_4)_2ZrMe^+$-μ-Me-$B(C_6F_5)_3^-$ (250 ms); *rac*-$Me_2Si(Ind)_2ZrMe^+$-μ-Me-$B(C_6F_5)_3^-$ (250 ms); *rac*-Me_2Si(2-Me-$Ind)_2ZrMe^+$-μ-Me-$B(C_6F_5)_3^-$ (250 ms); *rac*-Me_2Si(2-Me-Benz[*e*]-$Ind)_2ZrMe^+$-μ-Me-$B(C_6F_5)_3^-$ (350 ms); and *rac*-Me_2Si(2-Me-4-^{t}Bu-$C_5H_2)_2ZrMe^+$-μ-MeB$(C_6F_5)_3^-$ (20 ms).

Crystal Structure Determination. Crystallization of *rac*-Me_2Si(2-Me-4-^{t}Bu-$C_5H_2)_2ZrMe^+$-μ-MeB$(C_6F_5)_3^-$ by slow evaporation of a benzene solution in a glovebox gave yellow monoclinic prisms with approximate size of 0.4 × 0.4 × 0.4 mm. Crystal data were collected in the θ-range of 2−27° at 236 K, using a Siemens P4 diffractometer and Mo Kα radiation (λ = 0.71073 Å): space group $P2_1/n$, a = 14.784(2) Å, b = 20.149(4) Å, c = 18.810(5) Å, β = 100.70(2), Z = 4, V = 5505(2) Å^3, D_{calcd} = 1.436 g/cm^3, μ = 0.311 mm^{-1}, and F(000)=2444. A total of 12560 reflections were collected, of which 10816 were independent and 6320 reflections had $I > 2\sigma(I)$. The structure was solved by direct methods and refined with the SHELXL 93 program package.[20] All non-hydrogen atoms were refined anisotropically. The positions of the hydrogen atoms were calculated and refined with fixed isotropic U using the riding model technique. The final agreement factors were $R(F)$ = 9.65% and $R_w(F^2)$ = 23.0% ($w^{-1} = \sigma^2(F^2) + (0.0879P)^2 + 50.35P$, with $P = (F^2_{obs} + 2F^2_{calc})$). The Goodness-of-Fit was 1.052. Crystallographic data for the structure obtained have been deposited with the Cambridge Crystallographic Data Centre as supplementary publication CCDC 134808. Copies can be obtained, free of charge, on application to CCDC, 12 Union Road, Cambridge CB2 1EZ, UK (fax +44 1223 336033; e-mail deposit@ccdc.cam.ac.uk).

Acknowledgment. We thank Ms. Anke Friemel for excellent technical assistance with 2D-NMR measurements and Dr. Dmitri Babushkin for valuable comments and suggestions. For gifts of chemicals we thank Dr. Jürgen Suhm, Kunststoff-Laboratorium, BASF AG, and Dr. Carsten Bingel, Axiva Research and Technologies GmbH. Support of this work by BMBF, BASF AG, Fonds der Chemischen Industrie and funds of the University of Konstanz is gratefully acknowledged.

JA003531W

(20) Sheldrick, G. M. *SHELXS-86, SHELXL-93*; University of Göttingen, 1993.